

Isothermal and Non-Isothermal Crystallization of Poly(L-lactic acid)/Poly(butylene terephthalate) Blends

Maria Laura Di Lorenzo, Paolo Rubino, Mariacristina Cocca

Consiglio Nazionale delle Ricerche, Istituto di Chimica e Tecnologia dei Polimeri - c/o Comprensorio Olivetti - Via Campi Flegrei, 34-80078 Pozzuoli NA, Italy

Correspondence to: M. L. Di Lorenzo (E-mail: dilorenzo@ictp.cnr.it)

ABSTRACT: Isothermal and non-isothermal crystallization kinetics of poly(L-lactic acid)/poly(butylene terephthalate) (PLLA/PBT) blends containing PLLA as major component is detailed in this contribution. PLLA and PBT are not miscible, but compatibility of the polymer pair is ensured by interactions between the functional groups of the two polyesters, established upon melt mixing. Crystal polymorphism of the two polyesters is not influenced by blending, as probed by wide-angle X-ray analysis. The addition of PLLA does not affect the temperature range of crystallization kinetics of PBT, nor the crystallinity level attained when the blends are cooled from the melt at constant rate. Conversely, PBT favors crystallization of the biodegradable polyester. The addition of PBT results in an anticipated onset of crystallization of PLLA during cooling at a fixed rate, with a sizeable enhancement of the crystal fraction. Isothermal crystallization analysis confirmed the faster crystallization rate of PLLA in the presence of PBT. © 2014 Wiley Periodicals, Inc. *J. Appl. Polym. Sci.* **2014**, *131*, 40372.

KEYWORDS: blends; crystallization; differential scanning calorimetry (DSC); Biopolymers & renewable polymers

Received 12 July 2013; accepted 31 December 2013

DOI: 10.1002/app.40372

INTRODUCTION

Poly(L-lactic acid) (PLLA) is a biodegradable and biocompatible thermoplastic polyester produced from renewable sources.^{1–4} It is widely used for biomedical and packaging applications because of its excellent optical properties and very low toxicity.^{5,6}

PLLA can be degraded in natural environments by enzymatic or non-enzymatic hydrolysis.^{7–9} In both cases, biodegradation rate strongly depends on molecular weight and on crystal structure and morphology,¹⁰ which in turn are function of the thermal and mechanical history imparted during processing. As drawback, PLLA displays a low crystallization rate, which negatively affects its processability and properties. This led to throughout analysis of the crystallization kinetics of PLLA along the years, as efforts to improve its crystallization rate.⁷

Literature data indicate that three major strategies have been mostly followed to raise the crystallization kinetics of PLLA. A first possibility is to add a plasticizer which increases the polymer chain mobility and enhances the crystallization rate by reducing the energy required for the chain folding process.^{11–13} The molding conditions can also be tailored to tune crystallization rate and crystallinity, by varying molding temperature and time until the most favorable conditions are achieved.^{12,14} The

most common method, however, consists in the addition of a nucleating agent that lowers the surface free energy barrier toward nucleation and thus initiates crystallization at higher temperature upon cooling.¹⁵

One of the most effective nucleating agents for PLLA is the stereocomplex formed upon mixing poly(L-lactic acid) and poly(D-lactic acid) (PDLA).¹⁶ Most successful is the stereocomplex formed at a PLLA/PDLA 50/50 blend ratio, which has a melting temperature of 230°C, 50°C higher than that of the plain PLLA or PDLA. The overall crystallization rate of the stereocomplex is higher than that of pure PLLA or PDLA, due to faster nucleation and higher growth rate of stereocomplex spherulites, which sizably fastens the phase transition of PLLA.¹⁷

Talc appears at moment the most effective and cost-efficient nucleating agent. In the presence of 1% talc, the crystallization half-time of PLLA can be reduced by more than one order of magnitude.¹⁸ Biobased nucleants, like vegetable-based ethylene bis-stearamide, thermoplastic starch, and cellulose nanocrystals were also found to enhance the crystallization rate of PLLA, but with a lower efficiency compared to talc.^{19–21} Other compounds successfully used to increase crystallinity of PLLA include organically-modified montmorillonite clay,²² polyhedral oligomeric silsesquioxane,²³ and layered metal phosphonates.²⁴ However, the increase in crystallization rate attained with these

additives is relatively modest when compared to that observed with talc.¹²

Semicrystalline polymers were also successfully tested as nucleating agents for PLLA. It was reported that blending with poly(ethylene glycol) (PEG) can accelerate crystallization of PLLA.^{25–27} Similarly, poly(ϵ -caprolactone) (PCL) was found to enhance nucleation rate of PLLA.²⁸

As an attempt to improve the crystallization rate of poly(L-lactic acid), we propose to blend it with another polyester, namely poly(butylene terephthalate) (PBT). Poly(butylene terephthalate) is a widely used polyester with a very high crystallization rate, and it crystallizes at temperatures higher than the melting point of PLLA.^{29–31} Therefore crystallization of PLLA occurs in the presence of already grown PBT crystals, which may in principle promote nucleation of PLLA, enhancing its crystallization kinetics. Since crystallization kinetics in polymer blends is strictly related to miscibility of the components and to the phase structure, a detailed preliminary investigation on PLLA/PBT blends containing PLLA as major component was conducted, and results detailed in a companion publication.³² Briefly, PLLA and PBT are not miscible, but display compatibility due to the establishment of interactions between the functional groups of the two polyesters upon melt mixing. Electron microscopy analysis revealed that in the blends containing up to 20% of poly(butylene terephthalate), PBT particles are finely dispersed within the PLLA matrix, with a good adhesion between the phases. The PLLA/PBT 60/40 blend presents a co-continuous multi-level morphology, where PLLA particles, containing dispersed PBT units, are embedded in a PBT matrix. The varied morphology affects the mechanical properties of the material, as the 60/40 blend displays a largely enhanced resistance to elongation, compared to the blends containing lower amounts of PBT.³²

The influence of PBT on crystallization kinetics of PLLA is discussed in this contribution. It is shown that the addition of poly(butylene terephthalate) results in an anticipated onset of crystallization of PLLA upon cooling and a faster isothermal crystallization kinetics. Moreover, at parity of thermal history, in the presence of PBT, poly(L-lactic acid) has a much higher degree of crystallinity than the plain polymer, as detailed below.

EXPERIMENTAL PART

Materials

Poly(butylene terephthalate) (PBT) with melt flow index 20 g/min was purchased from Sigma-Aldrich Corp. Poly(L-lactic acid) (PLLA), grade name 4032D containing 1.5% D-lactic acid, was provided by NatureWorks LLC.

Before melt mixing, PBT was dried in a vacuum oven at 120°C for 16 h, and PLLA in vacuum oven at 80°C for 4 h.

Blend Preparation

PLLA/PBT blends were prepared by melt mixing in a Brabender-like apparatus (Rheocord EC of Haake Inc.) at 250°C and 64 rpm for 6 min. Binary blends with PLLA/PBT 100/0, 90/10, 80/20, 60/40 wt/wt were prepared.

The influence of processing conditions on thermal degradation of PLLA is detailed in Ref. 32.

Preparation of Compression-molded Sheets

The PLLA/PBT blends prepared in the Brabender-like apparatus were compression-molded with a Collin Hydraulic Laboratory Forming Press P 200 E at a temperature of 250°C for 2 min, without any applied pressure, to allow complete melting. After this period, a load of about 0.5 ton was applied for 2 min, then the sample was cooled to room temperature by means of cold water circulating in the plates of the press.

Calorimetry

Isothermal and non-isothermal crystallization kinetics of PLLA/PBT blends was investigated using a Mettler DSC 822° calorimeter, Mettler-Toledo, equipped with a liquid-nitrogen accessory for fast cooling. The calorimeter was calibrated in temperature and energy using indium. Dry nitrogen was used as purge gas at a rate of 30 mL/min. A fresh sample was used for each analysis.

In order to set the structure for the analysis of crystallization kinetics, each sample was heated from 25 to 250°C at a rate of 30°C/min, then melted at 250°C for 2 min to erase previous thermal history. Isothermal crystallization experiment was performed after cooling the blends from 250°C at 30°C/min to the selected temperature (T_c). For the non-isothermal crystallization analyses, the samples were quickly cooled from 250 to 220°C at 30°C/min, to limit as much as possible the exposure to high temperatures, then cooled to 25°C at various rates, ranging from 0.5 to 4°C/min. After completion of crystallization, the blends were heated again at 20°C/min until complete melting.

Crystallization is an exothermic process, and the heat evolved during the phase transition may cause some local heating and thermal gradients within the sample. As a consequence, transitions can occur at temperatures that do not correspond to those detected by the instrumentation.^{33,34} The thicker the sample, the more critical this problem is. In order to reduce these problems, a sample mass of 3.0 ± 0.2 mg was used. Moreover, cooling rates not exceeding 4°C/min were used, as higher cooling rates imply a faster development of latent heat that may cause higher thermal lag during the transition with the used sample mass.

Optical Microscopy

Morphology of PLLA/PBT blends was investigated by optical microscopy, using a Zeiss polarizing microscope equipped with a Linkam TMHS 600 hot stage and a Scion Corporation CFW-1312C Digital Camera. A small piece of each blend was squeezed between two microscope slides, then inserted in the hot stage. The thickness of the squeezed sample was lower than 10 μ m.

The thermal treatments were identical to those used in calorimetry. Each sample was heated from 25 to 250°C at a rate of 30°C/min, melted at 250°C for 2 min to erase previous thermal history, cooled to 220° at 30°C/min to limit as much as possible the exposure to high temperatures, then cooled to 25°C at 4°C/min. A fresh sample was used for each analysis.

Wide Angle X-ray Analysis

The crystalline structure of PLLA/PBT blends was investigated by wide-angle X-ray diffraction analysis (WAXD). WAXD

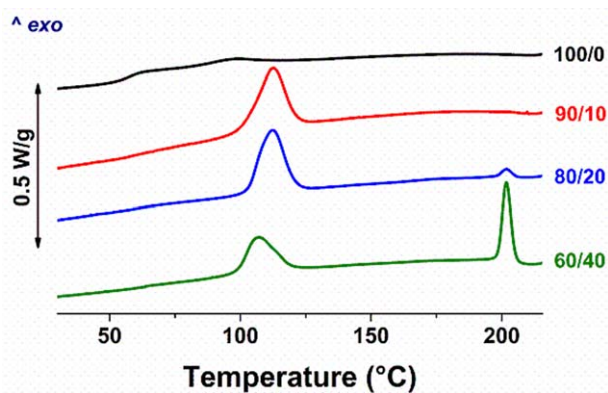


Figure 1. Heat flow rate plots of PLLA/PBT blends during non-isothermal crystallization from the melt at 4°C/min. [Color figure can be viewed in the online issue, which is available at wileyonlinelibrary.com.]

investigation was carried on compression-molded films by means of a Philips (PW 1050 model) powder diffractometer (Ni-filtered CuK α radiation) equipped with a rotative sample holder. The high voltage was 40 kV and the tube current was 30 mA.

Before WAXD analysis, the compression-molded film was non-isothermally crystallized upon cooling from the melt at 4°C/min, following the same thermal history detailed above. Non-isothermal crystallization of the films was carried out using a Mettler Toledo FP82HT Hot Stage coupled with a Mettler Toledo FP90 Central Processor.

RESULTS AND DISCUSSION

The DSC thermograms of the PLLA/PBT blends gained during cooling from the melt at 4°C/min are presented in Figure 1. Similar trends were obtained for the other cooling rates. Crystallization of PBT occurs at high temperatures, it starts around 208°C, and is completed at circa 197°C. The presence of PLLA seems not to affect crystallization of PBT, which takes place in the same temperature range, independently of blend composition.

The crystallization exotherm of PBT is barely visible in the 90/10 blend, and becomes progressively more intense with increasing PBT content. The onset of crystallization of PBT seems independent of PLLA content, indicating that nucleation kinetics of PBT is not affected by the presence of PLLA in the analyzed composition range, probably due to the very high nucleation density of PBT.²⁹ Normalization of the heat evolved during the phase transition with respect to PBT content indicates no variation of crystallization enthalpy with blend composition, as the heat of crystallization remains 41 ± 2 J/g for PLLA content ranging from 90 to 60%.

Since PLLA/PBT blends have phase-separation in the melt,³² crystallization of PBT occurs in the presence of non-crystallizable (at PBT crystallization temperature) PLLA segregated domains. Energy needs to be dissipated to perform rejection, engulfing or deformation of the biodegradable polyester. The overall effect depends on the values of the energy barriers that need to be overcome to reject, occlude and/or deform the

non-crystallizable domains.³⁵ It is likely that the hindrance introduced by the presence of dispersed domains is much smaller than the energy barriers for nucleation and growth of plain PBT crystals, and the overall effect of PLLA on crystallization of PBT is negligible.³⁶

Figure 1 also illustrates the effect of PBT on non-isothermal crystallization of PLLA. At the cooling rate of 4°C/min, the analyzed PLLA grade displays a weak and broad crystallization exotherm. In the presence of 10% of PBT, a much larger amount of PLLA chains organize into crystals, as revealed by the sizeable exothermic peak, centered at 112°C, in the DSC curve of the PLLA/PBT 90/10 blend. Similar exotherms are evident also in the DSC plots of the 80/20 and 60/40 blends, their reduced size is due to the decreasing amount of PLLA in the blends.

It is worth noting that in the PLLA/PBT 60/40 blend, the onset of crystallization is slightly delayed, compared to the 90/10 and 80/20 blends. The small shift of onset of crystallization is within the experimental uncertainty associated to DSC analysis, but the shape of phase transition exotherm varies with blend composition. In the 90/10 and 80/20 blends, the exotherms have sharp onset and termination, whereas in the 60/40 blend the beginning of the phase transition is gradual, with a fast termination. The shape of the DSC peak of the 90/10 and 80/20 blends is typical of crystallization occurring in the presence of a large number of preformed nuclei and fast termination due to crystallite impingement, whereas a gradual onset, as seen in the 60/40 blend, is expected in case of a broad distribution of nucleation times.³⁷ The varied nucleation efficiency of PBT is probably to be linked to the co-continuous morphology of this blend, shown below, since in the 60/40 blend the PLLA areas are dispersed within the PBT network, whereas in the 90/10 and 80/20 blends PLLA is the matrix that embeds the PBT particles.³²

From the solidification exotherms, the onset temperatures (T_{ons}) and the crystallization enthalpy (ΔH), normalized to PLLA content, were derived and results are illustrated in Figures 2 and 3, respectively. For every sample, with increasing the cooling rate

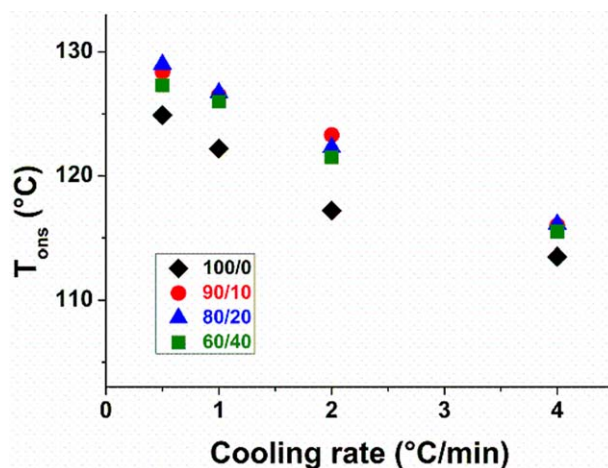


Figure 2. Onset temperature of crystallization of PLLA in PLLA/PBT blends as a function of cooling rate. [Color figure can be viewed in the online issue, which is available at wileyonlinelibrary.com.]

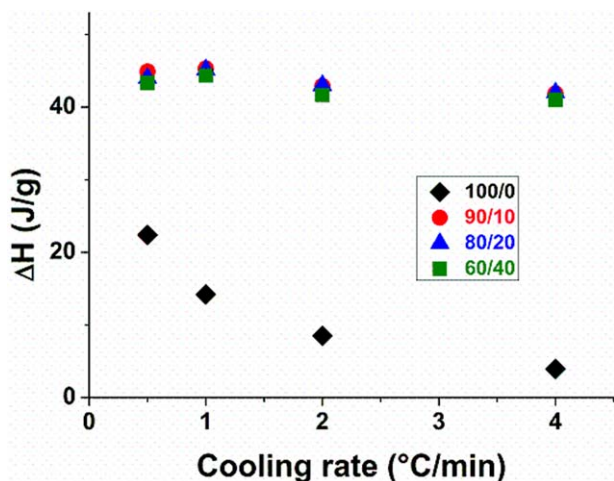


Figure 3. Enthalpy of crystallization of PLLA in PLLA/PBT blends as a function of cooling rate. [Color figure can be viewed in the online issue, which is available at wileyonlinelibrary.com.]

(χ) the crystallization curves shift to lower temperatures. At lower χ there is more time to overcome the nucleation barrier, so crystallization starts at higher temperatures, whereas at higher χ nuclei become active at lower temperatures.³⁸

For all the analyzed cooling rates, crystallization of plain PLLA initiates at temperatures well below those of the blends. The crystallization enthalpy of PLLA is also affected by the presence of PBT. For plain PLLA the heat evolved during the phase transition decreases from 22 J/g, measured upon cooling at 0.5°C, to 4 J/g determined at the cooling rate of 4°C/min. The decreased crystallinity of PLLA with cooling rate has been widely reported in the literature, being caused by its low crystallization rate.^{5,15} When PBT is added to PLLA, the enthalpy of crystallization, normalized to PLLA content, results much higher (43 ± 2 J/g) and independent of both composition and cooling rate. These data reveal the role of PBT on crystallization kinetics of PLLA. In the blends, crystallization of PBT upon cooling is completed at temperatures where the PLLA chains are in the melt state. The presence of PBT crystals can facilitate nucleation of PLLA spherulites, so that crystallization during cooling has an anticipated onset and starts at higher temperatures, as shown in Figure 2. The faster nucleation rate favors growth of a higher number of PLLA spherulites during cooling, which results in a largely enhanced crystal fraction of PLLA in the blends, as probed in Figure 3.

Morphology of PLLA/PBT blends after non-isothermal crystallization upon cooling at 4°C/min is presented in Figure 4.

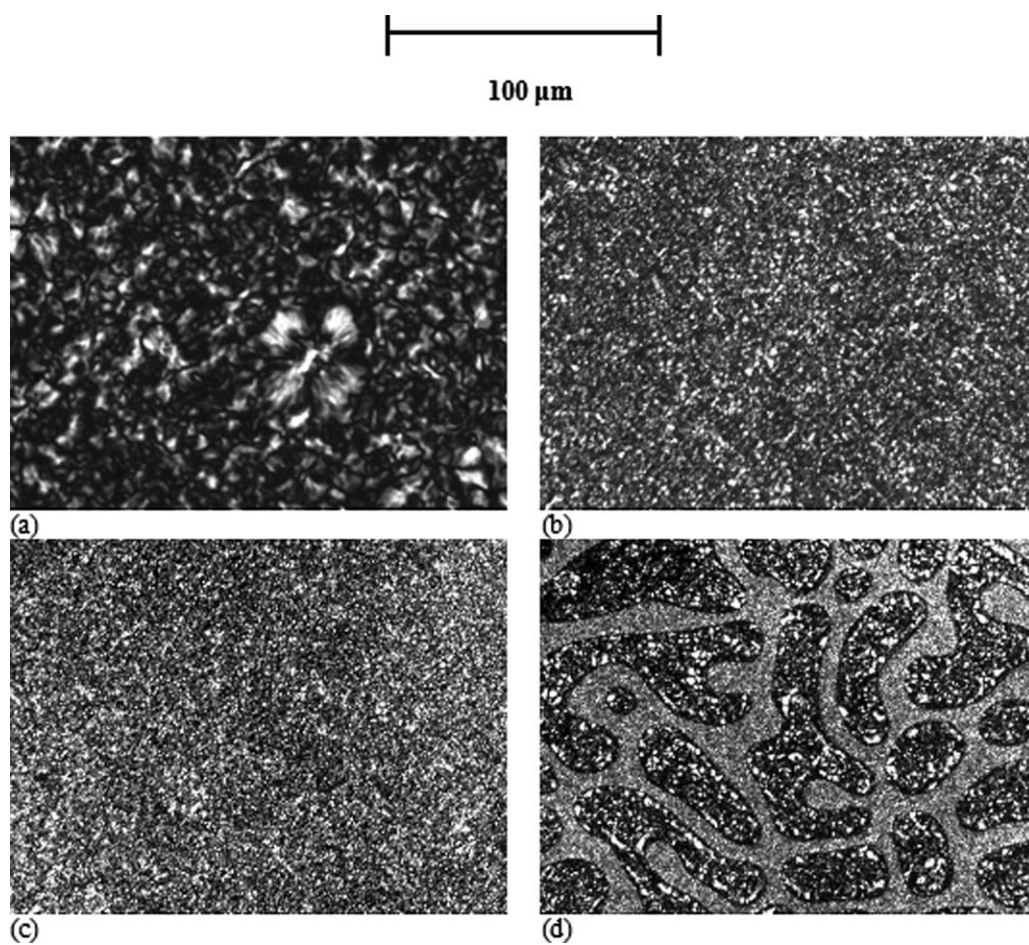


Figure 4. Optical micrographs (crossed polarizers) of PLLA/PBT blends after non-isothermal crystallization from the melt at 4°C/min: (a) 100/0; (b) 90/10; (c) 80/20; and (d) 60/40.

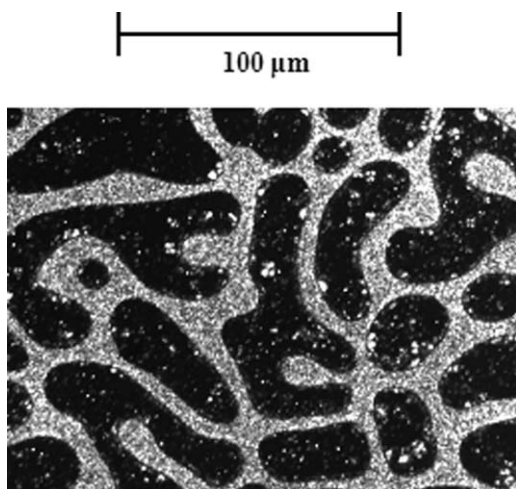


Figure 5. Optical micrographs (crossed polarizers) of PLLA/PBT 60/40 blend at 110°C during non-isothermal crystallization from the melt at 4°C/min.

Figure 4(a) illustrates plain PLLA crystallized according to a spherulitic morphology. Large and small spherulites are present. The appearance of spherulites of different sizes usually occurs when the nucleation process is time and temperature dependent.^{39,40} During cooling, at high temperatures the presence of few nuclei induces the formation of early spherulites that can grow to some extension, and these are the large spherulites present in this figure. Then, at lower temperatures, many nuclei result in simultaneous development of a huge number of spherulites that cannot expand to large extension like the early ones, as they impinge against each other.

Optical micrographs of the 90/10 and 80/20 blends after cooling to room temperature are shown in Figure 4(b,c), respectively. A very high number of small spherulites appear, which are almost indistinguishable upon optical microscopy analysis, as typical for PBT.²⁹ Also PLLA crystallites do not grow to large extension when they develop in the presence of already formed PBT crystals, which results in the morphology illustrated in Figure 4(b,c). In the 60/40 blend, whose optical micrograph is exhibited in Figure 4(d), the interconnected structure displays the presence of two types of crystallites: very small and poorly birefringent crystals in the co-continuous structure, made of PBT, and somewhat larger and more birefringent crystals in the embedded areas, where PLLA chains are present.

The increased nucleation density of PLLA upon addition of PBT is confirmed by the optical micrographs of Figure 4(a–c), where the size of the spherulites decreases with PBT content. In phase-separated blends, increase of nucleation density can be caused not only by the pre-existing crystals formed by the high-temperature crystallizing polymer, but also by decrease of the energy barrier for the formation of heterogeneous nuclei in contact with the interface between the dispersed phase and the matrix, also due to local orientation of the polymer chains.^{34,41}

The influence of the interphase on the increased nucleation density of PLLA spherulites was probed by analysis of the spherulite development during cooling. Figure 5 displays the polarized optical micrograph at 110°C of PLLA/PBT

60/40 blend, partially crystallized during cooling at 4°C/min. The 60/40 blend displays an interconnected multi-level morphology, where PLLA domains, containing dispersed PBT units, are embedded in a PBT matrix. At 110°C crystallization of PBT is complete, as evidenced by the bright birefringent co-continuous areas, whereas the phase transition of PLLA is far from completion. In the embedded areas, some increased density of growing PLLA spherulites occurs in correspondence of the interface between the PBT and PLLA phases, as shown in Figure 5. Previous analysis of the PLLA/PBT blends probed that melt mixing of the two polyesters induces the establishment of interactions between the functional groups of PLLA and PBT. The interacting PLLA and PBT chains are located at the interfacial regions of the blend, promoting compatibilization of the components.³² This probably favors weak chain alignment in correspondence of the interface, which facilitates growth of PLLA crystal nuclei. The decrease of the energy barrier for the formation of heterogeneous nuclei contacting with the interface, can also favor the heterogeneous nucleation of PLLA crystals.^{34,35} In the PLLA/PBT blends, these heterogeneous nuclei favor crystallization of PLLA, which starts at higher temperatures compared to plain PLLA.

Crystallization kinetics of PLLA/PBT blends was also investigated in isothermal conditions. A temperature range where all the analyzed compositions crystallize in a reasonable time was selected, to better compare the crystallization behavior of the various samples. Crystallization temperatures lower than 100°C were not taken into account, since, in the presence of PBT, crystallization of PLLA starts during cooling at 30°C/min before reaching the selected T_c for $T_c < 100^\circ\text{C}$. At $T_c \geq 100^\circ\text{C}$, a cooling rate of 30°C/min from 250°C to the desired T_c is sufficient to prevent crystallization during cooling. At this cooling rate, crystallization of PBT is completed at temperatures much higher than the melting point of PLLA. In other words, crystallization kinetics of PLLA occurs in the presence of already grown PBT spherulites. Analyses were conducted by differential scanning calorimetry to determine the overall crystallization rate of PLLA

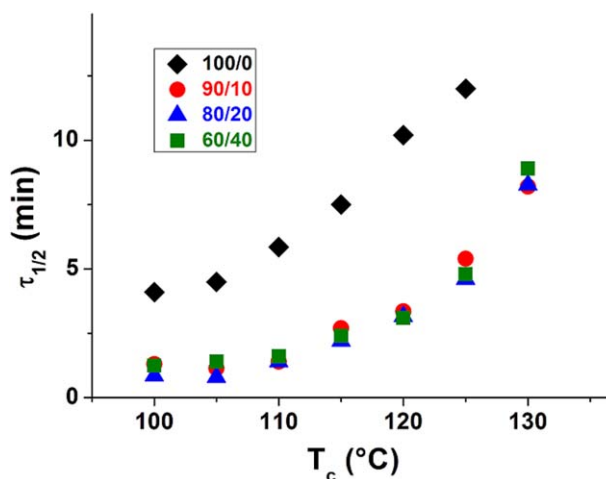


Figure 6. Half time of crystallization ($\tau_{1/2}$) as function of the isothermal crystallization temperature (T_c). [Color figure can be viewed in the online issue, which is available at wileyonlinelibrary.com.]

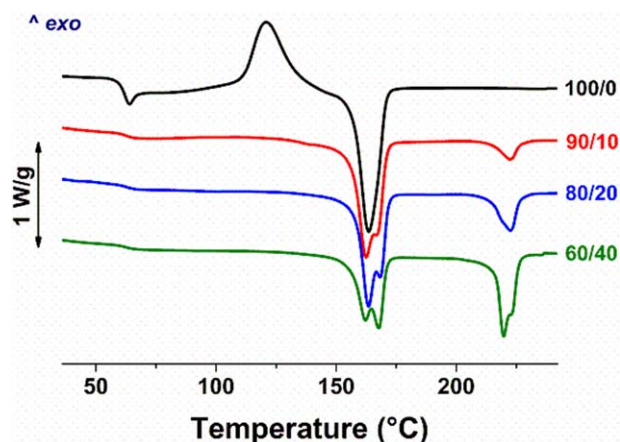


Figure 7. Heat flow rate plots of PLLA/PBT blends upon heating at 20°C/min, after non-isothermal crystallization from the melt at 4°C/min. [Color figure can be viewed in the online issue, which is available at wileyonlinelibrary.com.]

in the blends. Conversely, the growth rate of PLLA spherulites could not be easily determined by conventional optical microscopy methods,³⁶ due to the high density of nucleation of PBT spherulites, exemplified in Figures 4 and 5, which prevents reliable analysis of PLLA crystal growth rates.

The heat evolved during crystallization of PLLA was recorded as a function of time, and the fraction of material crystallized after a period of time t (X_t) was calculated from the ratio of the heat generated at time t and the total heat developed during the phase transformation. Plotting X_t against time, the half-time of crystallization ($\tau_{1/2}$), defined as the time needed for 50% the final crystallinity to develop, was obtained. The $\tau_{1/2}$ values of the analyzed PLLA/PBT blends are reported in Figure 6 as a function of temperature. As expected, in the analyzed range the phase transition rate decreases with T_c . More importantly, Figure 6 reveals that much shorter crystallization times are attained by PLLA in the blends, compared to the plain polymer, confirming the results of non-isothermal crystallization analyses, which revealed that the addition of PBT fastens crystallization of PLLA.

The influence of PBT on crystallization kinetics of PLLA is confirmed by analysis of the melting behavior. The DSC heating profiles of PLLA/PBT blends after non-isothermal crystallization from the melt at 4°C/min are presented in Figure 7. The influence of blending on glass transition is discussed in Ref. 32, hence is not repeated here. In plain PLLA a large cold crystallization exotherm occurs between about 96 and 140°C, followed by a single melting peak with a weak shoulder in the high temperature side. No cold crystallization exotherm can be detected in the PLLA/PBT blends containing 10–40% PBT, which only display two major endotherms, one at lower temperature, due to fusion of PLLA chains, and one at higher temperature, due to melting of PBT. The dual melting behavior of both polymers are well detailed in the literature and are caused by crystal polymorphism for PLLA, as well as by partial melting and recrystallization for both PBT and PLLA.^{42–45} The crystallinity values of the two polymers in the blends well compare with the data

gained upon cooling at the same rate (shown in Figure 3), and confirm the efficiency of PBT to enhance crystallization of PLLA.

As known from the literature, both PLLA and PBT can display crystal polymorphism. In PLLA four main different crystal modifications can develop, named α , β , γ , and ϵ forms, depending on preparation conditions. The α form of PLLA grows upon melt or cold crystallization, as well as from solution.^{46–48} Hot-drawing melt-spun or solution-spun PLLA fibers to a high-draw ratio leads to the β form,^{49–51} the γ form is obtained via epitaxial crystallization on hexamethylbenzene substrate,⁵¹ whereas the ϵ modification is a crystalline complex formed below room temperature in the presence of specific organic solvents such as tetrahydrofuran and N,N-dimethylformamide.⁵² Besides these three main crystal polymorphs, two disordered modification of the α form, named α' and α'' forms, were recently proposed for PLLA.^{48,53}

The effects of blend composition on crystal polymorphism of PLLA were investigated by WAXD analysis. Figure 8 exhibits the WAXD profiles of plain PLLA and of the three analyzed PLLA/PBT blends after non-isothermal crystallization from the melt at 4°C/min. For clarity, the profiles of the weak reflections are enlarged in Figure 7(b). Plain PLLA presents two strongest reflections at $2\theta = 16.7^\circ$ and 18.9° , corresponding to diffraction planes (110)/(200) and (203), and small diffraction peaks at 2θ of 12.7° , 14.9° , 22.4° , 23.9° , and 24.9° which are assigned to the reflections of (004)/(103), (010), (115), (016), and (206) planes

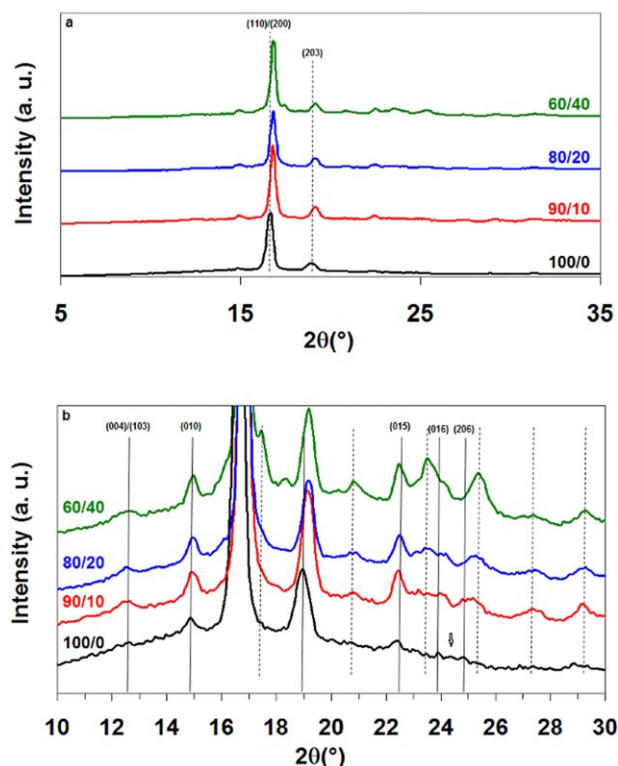


Figure 8. WAXD patterns of PLLA/PBT blends after non-isothermal crystallization from the melt at 4°C/min. [Color figure can be viewed in the online issue, which is available at wileyonlinelibrary.com.]

of α crystals, respectively.^{44,54} Besides the reflections ascribed to the α -form, neat PLLA exhibits a small peak at $2\theta = 24.4^\circ$, indicated in Figure 7(b) by an arrow, due to the α' -form.^{44,54}

The WAXD profiles of PLLA/PBT blends are characterized, in addition to the diffraction peaks typical of PLLA, also by the presence of diffraction peaks of PBT at 2θ Bragg's angle of 17.5° , 20.8° , 23.3° , and 25.4° .^{55–58} The intensity of the diffraction peaks of each component decreases with increasing the other polymer content in the blends, as expected. As it is possible to observe from Figure 7, the (110)/(200) and (203) reflections of the PLLA/PBT 90/10, 80/20, and 60/40 blends are located at higher 2θ than those of neat PLLA; this shift is independent of blend composition. These results suggest that the α -form crystals of PLLA are mainly developed in the PLLA/PBT blends, whereas in plain PLLA some sizeable fraction of α' crystals is present after crystallization at $4^\circ\text{C}/\text{min}$.^{48,51,54} Considering that in the presence of PBT, crystallization of PLLA occurs at higher temperatures, the results are in agreement with literature data, which report the development of a larger fraction of α crystals at higher crystallization temperature.^{44,54} This indicates that under the chosen experimental conditions (crystallization upon cooling from the melt at $4^\circ\text{C}/\text{min}$), the presence of PBT does not affect the crystal polymorphism of PLLA, which is solely determined by the temperature of phase transition, higher in the PLLA/PBT blends than in plain PLLA.^{54,59,60}

CONCLUSIONS

PBT crystallizes at temperatures much higher than PLLA, and its crystallization kinetics seems not affected by the presence of the biodegradable polyester, with reference to the investigated composition range and thermal histories. On the other hand, PBT remarkably affects the crystallization rate of PLLA, by promoting the onset of crystal growth. Upon cooling from the melt, crystallization of PLLA in PLLA/PBT blends is initiated at higher temperatures compared to plain PLLA and the attained crystal fraction is sizably higher than in plain PLLA.

The enhancement of PLLA crystallization rate is confirmed by optical microscopy analysis, which reveals a much higher nucleation density in the blends, as well by the shape of the DSC exotherm associated to PLLA crystallization, which has a sharp onset in the PLLA/PBT blends, due to simultaneous growth of a large number of crystals. In plain PLLA, instead, only a weak and broad exotherm can be obtained upon crystallization from the melt at the same cooling rate, due to the slow and faint release of heat upon formation of a low number of growing crystals.

The faster crystallization rate of PLLA upon addition of PBT is rationalized taking into account that upon cooling PBT crystallizes at temperatures much higher than PLLA; in the blends poly(L-lactic acid) crystals grow in the presence of already crystallized PBT chains, which may act as nuclei for the growth of PLLA spherulites. Moreover, as PLLA and PBT are non miscible, local orientation of the polymer chains at the interface between the PLLA and PBT phases may favor chain alignment to form crystal nuclei, and may also lead to a decrease of the energy barrier for the formation of heterogeneous nuclei in contact

with the interface between the dispersed phase and the matrix, which may also contribute to fasten nucleation of PLLA crystals.

The reported data indicate that addition of an immiscible semi-crystalline polymer with a high crystallization rate and high crystallization temperature is a successful novel strategy to enhance crystallization kinetics of poly(L-lactic acid), as PLLA based blends containing poly(butylene terephthalate) display considerable improvements in both crystallization rate and crystallinity, compared to plain PLLA.

REFERENCES

1. Bogaert, J. C.; Coszac, P. P. *Macromol. Symp.* **2000**, *153*, 287.
2. Hashima, H.; Nishitsuji, S.; Inoue, T. *Polymer* **2010**, *51*, 3934.
3. Di Lorenzo, M. L. *Eur. Polym. J.* **2005**, *41*, 569.
4. Saeidlou, S.; Huneault, M. A.; Li, H.; Park, C. B. *Progr. Polym. Sci.* **2012**, *37*, 1657.
5. Darder, M.; Aranda, P.; Ruiz-Hitzky, E. *Adv. Mater.* **2007**, *19*, 1309.
6. Nair, L. S.; Laurencin, C. T. *Progr. Polym. Sci.* **2007**, *32*, 762.
7. Fisher, E. W.; Sterzel, H. J.; Wegner, G. *Kolloid Z Z Polym.* **1973**, *251*, 980.
8. Iwata, T.; Doi, Y. *Macromolecules* **1998**, *31*, 2461.
9. Reeve, M. S.; McCarthy, S. P.; Downey, M. J.; Gross, R. A.; *Macromolecules* **1994**, *27*, 825.
10. Turner, J. F.; Riga, A.; O'Connor, A.; Zhang, J.; Collins, J. *J. Therm. Anal. Calor.* **2004**, *75*, 257.
11. Ljungberg, N.; Wesslén, B. *Biomacromolecules* **2005**, *6*, 1789.
12. Li, H.; Huneault, M. A. *Polymer* **2007**, *48*, 6855.
13. Xiao, H. Lu, W. Yeh, J. T. *J. Appl. Polym. Sci.* **2009**, *113*, 112.
14. Kawamoto, N.; Sakai, A.; Horikoshi, T.; Urushihara, T.; Tobita E., *J. Appl. Polym. Sci.* **2007**, *103*, 244.
15. Garlotta, D. *J. Polym. Environ.* **2001**, *9*, 63.
16. Ikada, Y.; Jamshidi, K.; Tsuji, H.; Hyon, S. H. *Macromolecules* **1987**, *20*, 904.
17. Tsuji, H.; Tezuka, Y. *Biomacromolecules* **2004**, *5*, 1181.
18. Ke, T.; Sun, X. *J. Appl. Polym. Sci.* **2003**, *89*, 1203.
19. Harris, A. M.; Lee, E. C. *J. Appl. Polym. Sci.* **2008**, *107*, 2246.
20. Li, H.; Huneault, M. A. *Intern. Polym. Proc.* **2008**, *23*, 412.
21. Pei, A.; Zhou, Q.; Berglund, L. A. *Compos. Sci. Techn.* **2010**, *70*, 815.
22. Ray, S. S.; Maiti, P.; Okamoto, M.; Yamada, K.; Ueda, K. *Macromolecules* **2002**, *35*, 3104.
23. Yu, J. Qiu, Z. *Thermoch. Acta* **2011**, *519*, 90.
24. Wang, S. Han, C.; Bian, J.; Han, L.; Wang, X.; Dong, L. *Polym. Int.* **2011**, *60*, 284.
25. Hu, Y.; Hu, Y. S.; Topolkarav, V.; Hiltner, A.; Baer, E. *Polymer* **2003**, *44*, 5681.

26. Wang, Z.; Wang, X.; Hsiao, B. S.; Andjelic, S.; Jamiolkowski, D.; Mcdivitt, J.; Fischer, J.; Zhou, J.; Han, C. C. *Polymer* **2001**, *42*, 8965.
27. Pluta, M. *Polymer* **2004**, *45*, 8239.
28. Sakai, F.; Nishikawa, K.; Inoue, Y.; Yazawa, K. *Macromolecules* **2009**, *42*, 8335.
29. Di Lorenzo, M. L.; Righetti, M. C. *Polym. Eng. Sci.* **2003**, *43*, 1889.
30. Righetti, M. C.; Di Lorenzo, M. L. *J. Polym. Sci., Part B: Polym. Phys.* **2004**, *42*, 2191.
31. Pyda, M.; Nowak-Pyda, E.; Mays, J.; Wunderlich, B. *J. Polym. Sci.: Part B: Polym. Phys.* **2004**, *42*, 4401.
32. Di Lorenzo, M. L.; Rubino, P.; Cocca, M. *Europ. Polym. J.* **2013**, *49*, 3309.
33. Monasse, B.; Haudin, J. M. *Coll. Polym. Sci.* **1986**, *264*, 117.
34. Di Lorenzo, M. L.; Cimmino, S.; Silvestre, C. *J. Appl. Polym. Sci.* **2001**, *82*, 358.
35. Bartczak, Z.; Galeski, A.; Martuscelli, E. *Polym. Eng. Sci.* **1984**, *24*, 1155.
36. Di Lorenzo, M. L. *Progr. Polym. Sci.* **2003**, *28*, 663.
37. Di Lorenzo, M. L.; Wunderlich, B. *J. Therm. Anal. Calor.* **1999**, *57*, 459.
38. Di Lorenzo, M. L.; Silvestre, C. *Progr. Polym. Sci.* **1999**, *24*, 917.
39. Wunderlich, B. *Macromolecular Physics, Vol. 1, Crystal Structure, Morphology, Defects*; Academic Press, Inc.: New York, **1973**.
40. Sajkiewicz, P.; Di Lorenzo, M. L.; Gradys, A. *e-Polymers* **2009**; article number 085.
41. Bartczak, Z.; Martuscelli, E.; Galeski, A. In *Polypropylene: Structure, Blends and Composites*; Karger-Kocsis, J., Ed.; Chapman & Hall: London **1995**; Vol. 2, Chapter 2, p 25.
42. Righetti, M. C.; Di Lorenzo, M. L.; Angiuli, M.; Tombari, E. *Macromolecules* **2004**, *37*, 9027.
43. Di Lorenzo, M. L.; La Pietra, P.; Errico, M. E.; Righetti, M. C.; Angiuli, M. *Polym. Eng. Sci.* **2007**, *47*, 323.
44. Zhang, J.; Tashiro, K.; Tsuji, H.; Domb, A. J. *Macromolecules* **2008**, *41*, 1352.
45. Di Lorenzo, M. L.; Cocca, M.; Malinconico, M. *Thermoch. Acta* **2011**, *522*, 110.
46. Alemán, C.; Lotz, B.; Puiggali, J. *Macromolecules* **2001**, *34*, 4795.
47. Sasaki, S.; Asakura, T. *Macromolecules* **2003**, *36*, 8385.
48. Pan, P.; Inoue, Y. *Progr. Polym. Sci.* **2009**, *34*, 605.
49. Hoogsteen, W.; Postema, A. R.; Pennings, A. J.; ten Brinke, G. *Macromolecules* **1990**, *23*, 634.
50. Puiggali, J.; Ikada, Y.; Tsuji, H.; Cartier, L.; Okihara, T.; Lotz, B. *Polymer* **2000**, *41*, 8921.
51. Pan, P.; Zhu, B.; Kai, W.; Dong, T.; Inoue, Y. *J. Appl. Polym. Sci.* **2008**, *107*, 54.
52. Marubayashi, H.; Asai, S.; Sumita, M. *Macromolecules* **2012**, *45*, 1384.
53. Marubayashi, H.; Akaishi, S.; Akasaka, S.; Asai, S.; Sumita, M. *Macromolecules* **2008**, *41*, 9192.
54. Di Lorenzo, M. L.; Cocca, M.; Malinconico, M.; Frezza, V. *Eur. Polym. J.* **2011**, *47*, 1073.
55. Deshmukh, G. S.; Pathak, S. U.; Peshwe, D. R.; Ekhe, J. D. *Bull. Mater. Sci.* **2010**, *33*, 277.
56. Yokouchi, M.; Sakakibara, Y.; Chatani, Y.; Tadokoro, H.; Tanaka, T.; Yoda, K. *Macromolecules* **1976**, *9*, 266.
57. Liu, J.; Geil, P. H. *J. Macromol. Sci. – Phys.* **1997**, *B36*, 263.
58. Desborough, I. J.; Hall, I. H. *Polymer* **1977**, *18*, 825.
59. Pan, P.; Kai, W.; Zhu, B.; Dong, T.; Inoue, Y. *Macromolecules* **2007**, *40*, 6898.
60. Zhang, J.; Duan, Y.; Sato, H.; Tsuji, H.; Noda, I.; Yan, S.; Ozaki, Y. *Macromolecules* **2005**, *38*, 8012.